Sensors & Transducers, Vol. 184, Issue 1, January 2015, pp. 26-38

www.sensorsportal.com

Sensors & Transducers

http://www.sensorsportal.com

A Highly Automated, Wireless Inertial Measurement Unit Based System for Monitoring Gym-Based Push-Start Training Sessions by Bob-Skeleton Athletes

Mark GAFFNEY, Dr. Michael WALSH, Brendan O'FLYNN, Dr. Cian Ó MATHÚNA

Tyndall National Institute, University College Cork, Cork, Ireland
Tel.: +353-21-490-4023, 4440, 4041, 4350, fax: +353-21-490-4880
E-mail: mark.gaffney@tyndall.ie, michael.walsh@tyndall.ie, brendan.oflynn@tyndall.ie, cian.omathuna @tyndall.ie

Received: 14 November 2014 /Accepted: 15 December 2014 /Published: 31 January 2015

Abstract: Wireless Inertial Measurement Units (WIMUs) are increasingly used to improve our understanding of complex human motion scenarios. In sports this allows for more valid coaching, selection and training methods leading to improved athletic performance. The Push-Start in the Winter Olympic sport of Bob-Skeleton is poorly understood but believed to be critical to performance. At the University of Bath a piece of gym-based equipment called the "Assassin" used by athletes to practice the Push-Start was instrumented with a custom WIMU system to investigate this motion regime. A test subject performed 36 runs, comprising 3 runs at each of 12 combinations of 3 Incline and 4 Weight settings. A developed algorithm automatically identified valid data-files, extracted the Pushing-Phase Acceleration data, and estimated sled Velocity and Displacement. The average velocities derived from an existing Light-Gate and WIMU data-files were comparable, with an average Root Mean Squared Error of 0.105 meters per second over the 52 valid WIMU data-files identified, covering 11 of the 12 Weight and Incline settings. Additional investigation of WIMU data revealed information such as: step count; track incline; and whether weights had been added could be determined, although further verification and validation of these features are required. Such an automated WIMU-based system could replace performance monitoring methods such as Light-Gates, providing higher fidelity performance data, additional information on equipment setup with lower-cost and greater ease-of-use by coaches or athletes. Its portable and modular nature also allow use with other training scenarios or equipment, such as using additional on-body WIMUs, or use with outdoor and ice-track sleds, enabling performance monitoring from the gym to the ice-track for improved candidate selection, comparison and training in Bob-Skeleton and other ice-track based sled sports.

Keywords: Wireless Inertial Measurement Unit, Accelerometer, Bob-Skeleton, Sled, Error Correction, Performance Monitoring.

1. Introduction

Bob-Skeleton is a Winter Olympics ice-track sledding sport – as are the more well-known events of Bob-sleigh, Luge and Toboggan – where a single athlete rides an open sled in a face-forward, prone manner. Each run begins with the Push-Start, which requires the athlete to sprint from stationary, in a

crouched position, accelerating to maximum velocity, over a short distance (~ 30-45 m), while pushing a heavy sled (~ 30-40 kg), before "Loading" (i.e. transitioning), then Riding the sled through a series of turns on tracks that are up to 1.5 km long (Fig. 1).

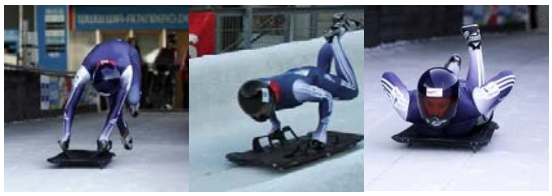

Fig. 1. The 3 Stages of a Bob-Skeleton Start (from left to right) Pushing, Loading, and Riding.

The sport is highly competitive, with the top times over the roughly 90 second run duration often within a fraction of a second of each other. While high velocity at the end of the Push-Start region is generally believed to be the most crucial aspect of final race time [1-2], this motion regime is poorly understood. A combination of the sport's small size and difficulty in accessing ice-tracks, is likely responsible for the lack of detailed Push-Start data and published studies. Relevant publications often rely on problematic data sources, such as: official timing (which ignores the first 15 meters) [1], [3-5]; alternative single interval timing (which hampers direct comparison, or understanding of subtle changes) [6-7]; or use complex and costly data gathering systems (limiting widespread use) [8-10].

As such, we set out to develop an easy-to-use, portable system that can provide high-quality sled velocity data. Ideally "On-Ice" performance would be investigated, however "Dry-Land" methods are more likely to be used for selection, comparison and training of Bob-Skeleton athletes [11-13] – especially for new athletes or in countries without a well-established amateur Bob-Skeleton system or easy access to ice-tracks – so initial system development and data gathering used such facilities at the University of Bath [14-15].

The "Assassin – Horizontal Power Trainer" is an indoor, gym-based Push-Start training tool. It consists of a sled which runs along a pair of parallel straight rails, allowing a 3 meter Free Travel Length before impacting the buffers, it also allows weights to be added to the sled and the track incline angle to be adjusted from horizontal to change the pushing effort required of the athlete; a Light-Gate pair provides quantified performance data; (see Fig. 2 and Fig. 3).

Wireless Inertial Measurement Units (WIMUs) are small electronic devices containing sensing elements, similar to those in smart-phones (i.e., Accelerometers, Gyroscopes, and Magnetometers), along with supporting components, which can act as un-tethered motion sensors. A custom WIMU system was built on the Tyndall 25 mm Mote Micro-System platform as part of on-going work on human motion capture for health and sports applications [16-21]; with laboratory calibration performed during assembly [22]. These were attached to the Assassin Sled for Push-Start data gathering.

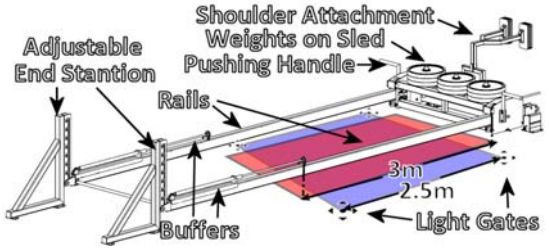

Fig. 2. Assassin Diagram with 3 m Free Travel Length (red) and 2.5 m Timed Region (blue).

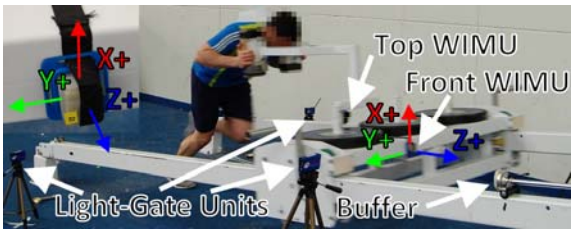

Fig. 3. Attached WIMU (inset) and Assassin In-Use.

The main desired output of this system was sled velocity, as this was considered the key performance determining feature of a good Push-Start. An automatic process was developed to accurately determine sled velocity using WIMU data recorded from an Assassin run [14]. The WIMU system's high sampling rates provided detailed information on how velocity develops from standstill, which could be crucial in determining the subtle effect of changes to training, warm-up and pushing technique and giving a competitive edge.

WIMU derived sled velocity results were validated by comparing to an existing Light-Gate system. An initial target of accuracy within 0.1 meters per second was set as this was considered the threshold for indicating notable differences in performance levels and effectiveness of coaching interventions.

Detection or identification of any additional features of interest from the WIMU sensor data was also attempted as these may help identify changes to technique or allow for more automated logging of a training session.

In Section 2, "Data Sources and Method", the equipment, setup, subject and procedure are described. Section 3, "Analysis", describes the stages of a run from the sensor data, focusing on the segmentation and processing of sled acceleration data during the Pushing Phase, as well as how to improve results using drift correction methods as included in the automatic adaptive integration process. Section 4,

"Results", details the average velocity value output generated for each data-file, how these are combined to quantify overall performance of the WIMU system against the Light-Gate as well as the potential for determining additional useful information. Sections 5, 6 & 7 contain the "Discussion", "Conclusion" and "Future Work" sections that contextualize the results, the effect of this work and detail how it can be developed from this point.

2. Data Sources and Method

All testing was performed in a single session, using the same subject, with a range of equipment settings and repeated runs at each setting. WIMU sensor output, Light-Gate timing, Assassin setting, and physical measurement data were recorded during this session and are described in further detail below.

2.1. WIMUs, Location and Orientation

Two identical WIMUs were configured to provide sensor data as follows: Accelerometer – Rate 256 Hz, Range ±16 g; Gyroscope – Rate 256 Hz, Range ±2000°/s; Magnetometer – Rate 50 Hz, Range ±1 Ga. The effective sampling rate varied, being dependent on un-predictable events such as wireless packet loss. Data was streamed via 802.15.4 compatible radio at 2.45 GHz to a Base-station connected to a notebook computer. APIs and scripts – written in the Python programming language (python.org) – enabled WIMU configuration, as well as gathering, processing and logging to Hard Drive of sensor data. All sensor data were converted to real world units – using previously gathered laboratory calibration values stored on each WIMU – before being written to file.

Two WIMUs (Front and Top) were placed into 3D-printed holders before being secured to the metal spars of the moveable sled, with similar orientation, using Velcro-elastic straps and tape as shown in Fig. 3. The Z-axis of the WIMU was aligned with the direction of forward motion of the sled as this provided the clearest Line-of-Sight between WIMU antenna (located on the +Z face of the WIMU) and Base-Station (located on a table to the side of the Assassin). The X-axis was aligned with the gravity vector for the Assassin at a 0° Incline setting. Using multiple WIMUs provided redundancy and allowed for investigation of the effect of WIMU placement.

Of note, the Front WIMU was secured directly to a horizontal member of the sled, whereas the Top WIMU was secured to a vertical member of the padded shoulder attachment the athlete pushed against. The sled ran on the rails using several small rubber wheels on the top and bottom of each rail member, this allowed some tilting of the sled as the athlete addressed it or pressed against it. The shoulder attachment was also secured to the sled using bolts which also had some "play", allowing additional movement relative to the sled. The effect of the different WIMU positions and relative motions due to such mechanical play will be discussed later.

2.2. Other Equipment and Data Sources

A Brower "Timing Centre" Light-Gate system [23] – consisting of 2 emitters and 2 receivers on approximately 1m tall tripods forming a 2 beam system – was positioned to cover approximately the central 2.5 meter portion of each run, indicated using X-shaped marks on the ground (See Fig. 2 and Fig. 3). The distance between these X-shaped marks for positioning the Light-Gates and heights of the rail at each end for the different Incline settings used were measured using a surveyor's tape, providing results considered accurate to the nearest centimeter. Nominal Incline angles and Free Travel Length were provided on technical drawings of the Assassin made available as part of the investigation.

2.3. Subject

A fit male was used as the test subject, representing a potential Bob-skeleton athlete undergoing selection. He was familiar-with and trained-in the use-of the Assassin, and was part of on-going sports science and performance research programs at the University of Bath and UK Sports which these tests were a part of. The purpose, procedures and equipment were explained to him and he had opportunity to ask questions or suggest changes to the procedure. He was also allowed to warm-up, take breaks, perform practice runs or stop the testing at his discretion.

2.4. Procedure

36 test runs were planned, allowing for 3 runs at each combination of 3 nominal rail angles (including the minimum and maximum inclination i.e. 0, 4 and 7°), and 4 weight settings (0, 20, 40 and 60 kg). The test procedure was as follows:

1. Sled is at rest at starting point.
2. Check, Adjust & Note Weight & Inclination.
3. Reset WIMUs and Light-Gates.
4. Test subject proceeds when ready.
5. Stop WIMU recording after the end of run.
6. Note Light-Gate timing value.

3. Analysis

An initial manual review of the gathered WIMU data was used to establish appropriate processing strategies and identify consistent events or features of

interest. Filtering and graphing of the gathered WIMU data helped to identify such features and was performed using Microsoft's Excel Spreadsheet software (products.office.com/en-US/excel) or the "Numpy" (numpy.org) and "MatPlotLib" (matplotlib.org) numerical analysis and graphing libraries for Python. The Z-Accelerometer was the principle WIMU data of interest as it allowed for estimation of sled velocity and displacement. The identified features are described and illustrated in the text and Fig. 4 below with the abbreviations for each feature being used throughout the rest of the text.

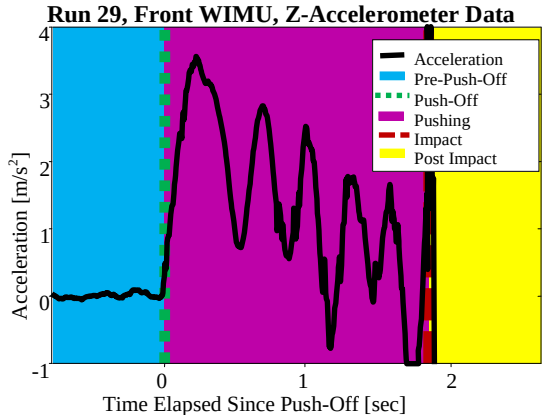

Fig. 4. Labelled Graph of Z-Accelerometer Output versus Time, showing the main features of an Assassin Run.

3.1. Assassin Run Z-Accelerometer Features

- Pre-Push-Off (PPO): Region with sled at rest at the start of the track; contains occasional motion artifacts due to the athlete addressing the sled.
- Push-off (PO): The start of Pushing-Phase, identified by a sudden rise in acceleration from PPO quiescent levels.
- Pushing-Phase (PP): Region lasting roughly 2 seconds, with large, cyclical, acceleration features.
- Impact Point (IP): A sudden large acceleration feature when the sled contacts the buffers, sensor saturation is common.
- Post Impact (PIP): The remaining data, often beginning with saturated severe oscillations.

3.2. Data from Other Sensors

Non-PP Z-Accelerometer data, as well as the output of the 8 other sensor data streams gathered by each WIMU were also of use and will be discussed later.

3.3. Sources of Drift & Error Correction

Theoretically it should be possible to combine instantaneous sled acceleration values to yield accurate sled Velocity and Displacement. However, the recorded WIMU derived Z-Accelerometer data is not a perfect representation of sled acceleration along the track. This is due to issues such as: misalignment; gravity effects; relative motion; finite sampling rates; limited sensor range; noise; and quantization error. Each time such data are integrated these errors compound. This is called Drift and it tends to increase over time as shown in Fig. 5 below.

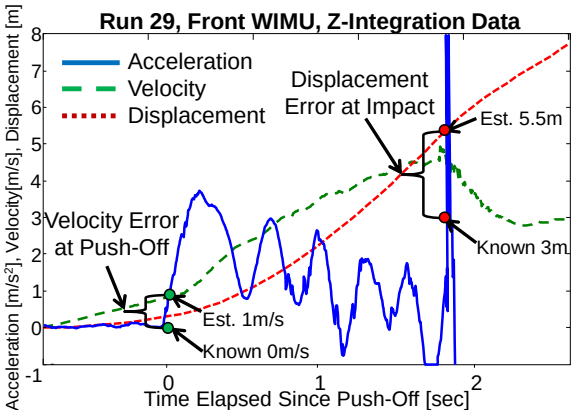

Fig. 5. Sample of Integration Errors at Push-Off and Impact for Run Without Drift Correction showing increasing Error.

Mitigation strategies are applied to the Z-Accelerometer data gathered from the Assassin runs, leading to significantly improved results as follows:

- Avoid integration of data where no motion of interest occurs or where sensor data is unreliable as these data do not contribute to or accurately represent sled forward motion – i.e. remove the PPO and PIP regions as the sled is effectively stationary and they contain extended quiescent periods and saturation respectively.
- Re-adjust sensor offsets for each Run & WIMU as these are highly liable to have changed from the previously determined values due to: orientation changes WRT to the gravity vector; temperature effects; voltage sensitivity; and sensor damage or aging. For this scenario, as we are mostly concerned with acceleration in the direction of sled motion, we can use knowledge of the track inclination angle, or the average PPO quiescent sensor value to determine initial offset values.
- Use known physical limits as integration constraints. In the Assassin scenario these are: Initial Velocity and Displacement values are 0 meters & 0 meters per second; Negative Velocity or Displacement values are not possible; and Displacement at IP equals the sled Free Travel Length (3 meters). Various key values which are known to be inaccurate can then be refined to yield integration results that meet these known physical limits.

- Re-estimate the integration period to account for differences between requested and effective sample rate. This can use individual sample-to-sample periods or an overall average based on number of samples obtained over a known duration.

While such methods could be performed "by-eye" or manually, an automated method is desirable to reduce subjective human variability and enable development of a self-contained high-accuracy performance monitoring system suitable for use by athletes and trainers.

3.4. Automated Sled Tracking Procedure

An automated analysis system was implemented in the Python programming language to track the motion of the sled from recorded Accelerometer data. It consists of several stages as described below and illustrated in the flowchart in Fig. 6: Pre-Processing; Impact Detection; Run Segmentation; Start Detection; Integration; and Evaluation versus the Light-Gate.

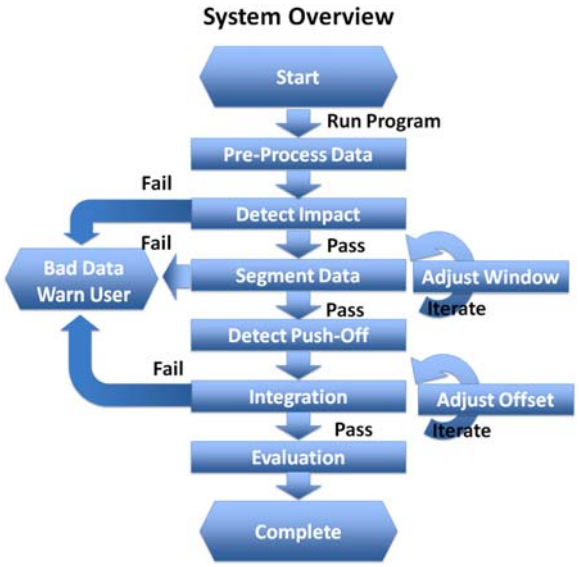

Fig. 6. Simplified Flowchart of Assassin Data Analysis Algorithm.

1. Pre-Processing – Data are prepared for subsequent analysis. WIMU sensor values are converted to appropriate units (e.g. Acceleration in 'g' to m/s^2), filtered and smoothed (for use in subsequent integration, segmentation, and feature detection stages). Data from other sources (such as Light-Gate timing, Assassin settings and physical measurements), are also combined for more complete logging or used to estimate values (such as expected Accelerometer Offset based on Nominal Incline setting) for later processing stages.

2. Impact Detection – The largest magnitude Acceleration features are identified as Impact Candidates. A threshold is used to check if these are suitably large, notifying the user and exiting processing of this WIMU file if no suitable candidates are found.

3. Segmentation – Contiguous Active and Passive regions of sensor data are identified using detection thresholds estimated from the variability of the most quiescent region of sensor data. From these, the Active region that contains sufficient data between its start and an Impact Candidate is identified as the PP. If segmentation is unsuccessful, new thresholds can be determined and segmentation re-attempted.

4. Push-Off Detection – The start of the identified active region is searched for a characteristic Acceleration peak, the beginning of this feature is considered the Push-Off.

5. Integration – Initial conditions are set, the offset is applied, period is determined and integration is performed based on the equations of motion to yield Sled Velocity and Displacement for each Accelerometer value. Comparing the estimated and known Displacement at IP allows for iterative refinement of the poorly known Sensor Offset to yield improved integration results.

6. Evaluation – The integrated WIMU data corresponding to the region between the Light-Gates is extracted from the estimated Sled Displacement values using the known Light-Gate positions. The WIMU derived Sled Average Velocity values within this region can then be calculated for comparison with Light-Gate derived values for validation of the Procedure.

3.5. Estimation of Full Run Duration

Ideally, the effective sample rate would be constant and equal to the requested sample rate, leading to simple determination of the integration period. However, as previously mentioned, the system's effective sample rate varies, being affected by unpredictable events such as wireless packet loss. Improved estimates can be made using per-sample times, or well-known sample counts over a specified duration; however at the time, the WIMU system lacked accurate per-sample time-stamping, preventing such direct estimations of effective integration period. As such, Light-Gate derived timing data was used instead of WIMU timestamps. However, the Light-Gates did not cover the full run, neglecting approximately the first and last 0.25 meter long regions of each run (Fig. 7).

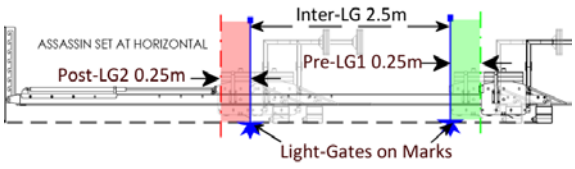

Fig. 7. Side view of Assassin showing pre- & post- Light-Gate un-timed regions (Green & Red respectively).

Displacements derived from preliminary WIMU

integration data from the 52 valid WIMU data-files, were used to identify those closest to the Light-Gates, i.e. displacements of 0.25 and 2.75 m. The samples between these were counted and combined with the Light-Gate derived time to estimate the effective sample rate and hence integration period. Gathering all the results (Fig. 8) allowed the Timed Region to be estimated as 67.7±1.9 % of the Full Run duration. This ratio of 0.677 allowed ready estimation of the integration period from the number of samples during the Pushing Phase and the Light-Gate duration.

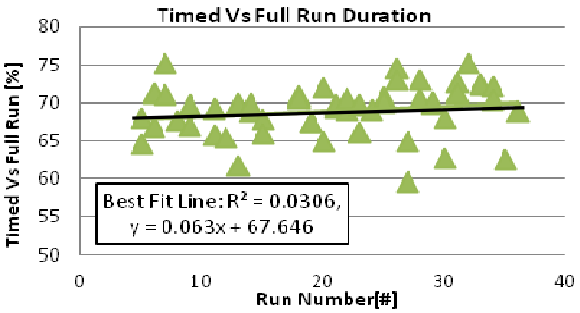

Fig. 8. Timed Region Duration Estimate from WIMU data.

3.6. Identification of Valid Data

Not all recorded WIMU data-files were of sufficient quality to yield reliable integration results. A fully automated system should be able to distinguish good and bad data-files to ensure only the most valid results are generated. Several data rejection conditions were identified, with suitable tests performed during analysis and warnings provided as follows:

1. "Missing Events in WIMU Data" – Recording started too late or finished too early, cutting off PO or IP, and causing failure during event detection stages.
2. "Missing Data from Other Sources" – Other essential data was un-available (i.e. Light-Gate).
3. "Excess Data Loss" – PP had less than 50 % of the data samples expected.

3.7. The Integration Process

An initial estimate of sensor offset is made based on the average value of the previously identified passive regions of sensor data in the PPO region (1) from the Segmentation stage. This initial offset is applied to each PP sensor sample to better estimate sled acceleration.

$$acc_{offset} = \frac{\sum_{k=0}^{N} acc_k}{N} [m/s^2], \quad (1)$$

for N Quiescent raw accelerometer samples, acc_k, in the Pre-Push-Off (PPO) Region.

A more representative integration period based on the effective sample rate is subsequently estimated. As mentioned above, using the previously determined ratio of Timed Region to Full Run durations (0.677), Light-Gate timing T_{LG}, and PP sample count i_{PP}, an improved period t, could be estimated as seen in (2).

$$t = \frac{T_{PP}}{i_{PP}} = \frac{T_{IP} - T_{PO}}{i_{IP} - i_{PO}} \approx \frac{T_{LG} / 0.677}{i_{IP} - i_{PO}}, \quad (2)$$

for Integration Period t, Time T and Sensor Sample i.

Using this period t, and the equations of motion, offset adjusted Acceleration data, a, from the PP can be used to estimate Velocity, v, (3) and Displacement, s, (4) for the n^{th} sensor sample since PO.

$$v_n = v_{n-1} + a_n t \quad (3)$$

$$s_n = s_{n-1} + v_{n-1} t + \tfrac{1}{2} a_n t^2 \quad (4)$$

Although the equations of motion above might seem the most logical choices to use for estimating Velocity and Displacement from Acceleration, in practice, rectangular integration is often used. Although the integration of Acceleration to Velocity (5) is functionally identical to the equation of motion (3), the integration to Displacement (6) is less computationally complex than its associated equation of motion (4). This makes the process more suitable for implementation on devices with limited processing power such as the Micro-controllers used in the WIMU.

$$v_n = \sum_{k=0}^{n} a_k t \quad (5)$$

$$s_n = \sum_{k=o}^{n} v_k t \quad (6)$$

Known and WIMU estimated Displacement at Impact are compared to each other and used to refine the Offset value using an iterative search process as explained in the C-style pseudo-code in Fig. 9 below.

3.8. Evaluation of Integration

The performance of the integration process was also evaluated by estimating the difference in WIMU and Light-Gate derived Average Velocity across the Timed Region. The Light-Gate Average Velocity was estimated using the equation of motion (7) by dividing the time displayed, by the nominal distance between the gates (i.e. 2.5 m). For the WIMU, the index of the first double integrated displacement values that met or exceeded 0.25 and 2.75 meters were identified, with all the corresponding Velocity values between these being combined using a simple numerical average.

```
WHILE( !complete && i<max_iteration ){
 IF( ABS(displ_error) >= target_accuracy ){
  IF( displ_error > 0 ){
   test_offset = offset - offset_step;}
  }ELSE{ // displ_error < 0
   test_offset = offset + offset_step;}
  z_vel = itegrate( z_acc, test_offset, period );
  z_displ=itegrate( z_vel, test_offset, period );
  impact_displ = z_displ[-1];
  new_error = impact_displ - target_displ;
  IF( ABS(new_error) < ABS(displ_error) ){
   offset = test_offset;     // update offset
   displ_error = new_error;} // update error
  offset_step /= 2;
  i++;
 }ELSE{ // ABS(displ_error) < target_accuracy
  complete=True ;}
}
```

Fig. 9. Iterative Sensor Offset Refinement.

The error for each data-file was estimated by subtracting the Light-Gate and WIMU derived Average Velocity values. To evaluate error over multiple data-files the Root Mean Squared Error (RMSE) (8) was used. This presents a more realistic idea of system accuracy compared to a simple average as it uses error magnitude, preventing over-estimations from counteracting under-estimations, and also takes into account the number of values available at each point giving less weight to data points with fewer values.

$$v_{avg\_nm} = (t_m - t_n)/(s_m - s_n), \quad (7)$$

$$RMSE = \sqrt{\frac{\sum_{t=1}^{n}(\hat{y}_t - y)^2}{n}}, \quad (8)$$

for n samples, of differences between a recorded value y and the t^{th} estimate of that value $\hat{y}_t$.

4. Results

Of the 36 runs, 2 WIMU data-files were corrupted giving 70 sets of useable WIMU data. Of these, 52 were determined to contain valid Z-Accelerometer PP data. All of these were segmented successfully on the first attempt. The iterative integration process used an initial step size of 10 m/s^2, and a maximum of 20 iterations, allowing for offset adjustment resolution of 9.5×10^{-6} m/s^2. An average of 12.17±0.98 sensor offset refinement iterations were required to reach the targeted Impact displacement value range of 3±0.005 m.

A composite scatter graph of results was generated for each WIMU data-file processed to allow rapid analysis of results. This showed Time on the X-Axis (as either seconds or samples since PO), with Acceleration, Velocity & Displacement on the Y-Axis. These 3 WIMU derived values were graphed as solid blue, dashed green and dotted red lines respectively. Additional items include: a black vertical line indicating the identified PO (dotted) and IP (Dashed), with dashed horizontal lines indicating Light-Gate derived average velocity (cyan) and Impact Displacement (blue). A shaded cyan block covered the timed region with its height indicating the WIMU derived Average Velocity. Of note, the red dotted Displacement line should cross the vertical black dashed IP line near its intersection with the horizontal blue 3 m line, indicating IP occurred at 3 meters. A good result was indicated if the shaded region's height (WIMU derived Average Velocity) was close to the horizontal dashed cyan line (Light-Gate derived Average Velocity).

4.1 Integrated Versus Light-Gate Velocities

Samples of the composite scatter graphs show the WIMU and Light-Gate derived Average Velocity over the timed region are very similar, differing by only 0.06 m/s in the example for Run 26 with the Front WIMU seen below (Fig. 10).

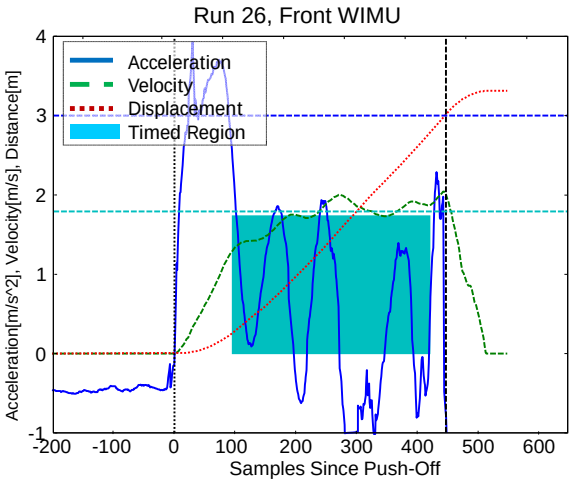

Fig. 10. Output for Run 26 showing Good Average Velocity Agreement between WIMU & Light-Gate Data.

This was not an isolated good result, as indicated by the summary of errors presented in Table 1 below. As described above, the RMSE value is far larger than the Average error but gives a more realistic idea of performance variability, being similar to the value of Standard Deviation.

Table 1. Combined Light-Gate versus WIMU Average Velocity Differences

Error [m/s]	*Avg*	*Std Dev*	*Max*	*Min*	*RMSE*
Top	-0.007	0.085	0.22	-0.124	0.084
Front	-0.002	0.062	0.178	-0.106	0.061
Both	-0.005	0.075	0.22	-0.124	0.074

To more readily visualize and identify performance or accuracy issues across the full range of Assassin settings, contour graphs were used. Weight and Incline settings are on the X & Y-axes respectively, with increasing values as you move to the upper right, and the actual graphed value of interest represented by changing colors ranging from high values in red to low values in blue. Gaps between values are filled and contours created using linear interpolation. Of note, white regions indicate no data is available and gray numbers at each location denote the number of results available and used at that combination of settings to produce the graphed value. The maximum and minimum values are also indicated with a black dot and associated text label.

Graphs of Light-Gate and WIMU derived mean Sled Average Velocity (See Fig. 11 and Fig. 12 respectively) show similar magnitudes and a trend for reduced velocity with increasing resistance as expected (i.e. increased Weight and steeper Incline leads to lower velocity).

The RMSE graph (See Fig. 13) shows the high level of agreement between the Light-Gate and WIMU results, with a maximum error of 0.105 m/s, and most results being well within the target accuracy level of 0.1 m/s across the wide range of equipment settings used. The yellow color in this contour graph corresponds to the targeted system agreement level or accuracy of 0.1 m/s, "redder" colors are performing worse, and "bluer" colors are performing better than this target. It should be noted that the contours used on the RMSE graphs are much closer than those on the previous mean Average Sled Velocity Graphs covering 0.01 and 0.1 m/s respectively.

4.2. Light-Gate Uncertainty

The Light-Gate derived Sled Average Velocity is not exact, as both the timing and distance measurements required have an associated uncertainty. The Light-Gate time data is provided on a handheld device screen in seconds with two places of decimals, as such estimated un-certainty is 0.01 seconds. The un-certainty in the distance travelled by the sled, due to errors in positioning the Light-Gates on 1 m tall tripods, was estimated at 0.02 meters. Additionally, inclination affects the actual distance travelled by the sled along the rails between the Light-Gates and depends on how they were positioned i.e. did the sled break the beams at the same point or at the same height above the ground? The difference between these was trigonometrically estimated as ±0.02 meters (2.519 or 2.48 meters respectively for the 2 extreme situations at the maximum Incline of 7°) (see Fig. 14). Adding these gives an overall maximum distance error estimate of ±0.04 meters. By combining the lower time with upper distance estimates and vice-versa, the un-certainty in Light-Gate Derived Sled Average Velocity was estimated as ranging from 0.066 to 0.115 meters per second (±2.3 % on average) (see Table 2).

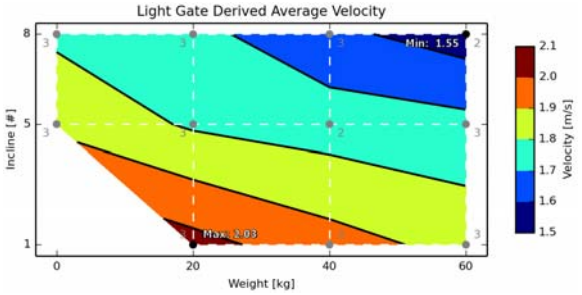

Fig. 11. Light-Gate derived Average Sled Velocity.

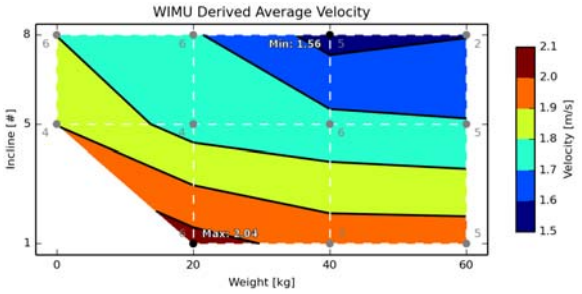

Fig. 12. WIMU derived Average Sled Velocity.

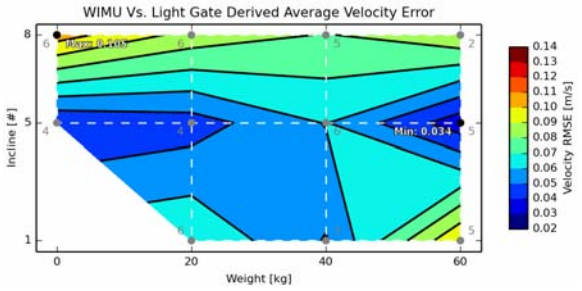

Fig. 13. RMSE of Sled Average Velocity for 2 Methods.

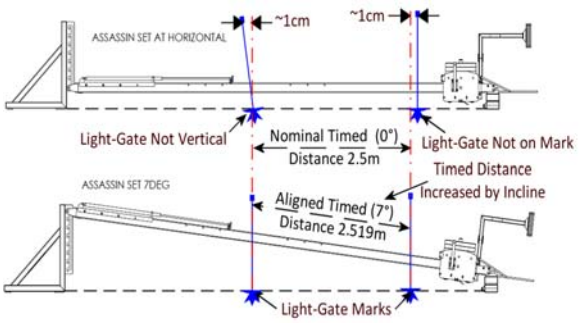

Fig. 14. Illustration of Light-Gates and Assassin from side Showing Sources of Timed Distance Un-certainty.

Table 2. Light-Gate Uncertainty Estimates.

For 2.5±0.04 m	Duration [sec]	Velocity [m/s]	Un-Certainty
Slowest	1.67±0.01	1.497±0.066	±2.199 %
Fastest	1.09±0.01	2.294±0.115	±2.518 %
Average	1.43±0.01	1.748±0.080	±2.300 %

4.3. Investigation of WIMU Placement

The use of two different WIMUs placed at different locations on the moving sled gave rise to the potential for different results due to differences in: inherent device performance; radio environment; attachment to structural member; and motion regime at each location. The data in Table 3 and example processed scatter graphs from Run 26 (see Fig 15) illustrate the overall and typical per-run differences between the two WIMUs.

Table 3. WIMU Performance Comparison.

WIMU	Valid Runs	Assassin Settings	Effect. Rate	Error >0.1 m/s	RMSE
Top	28/35	11/12	85 %	8/28	0.08 m/s
Front	24/35	9/12	78 %	2/24	0.06 m/s

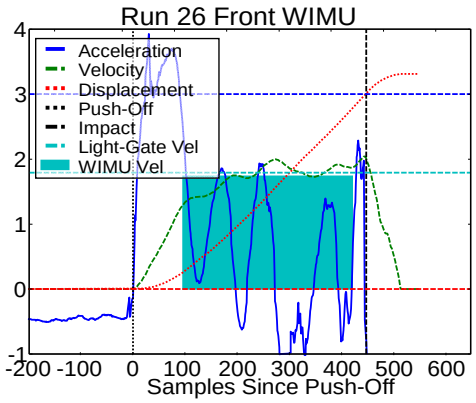

Fig. 15. Front WIMU has smoother acceleration.

The Top WIMU was located further back and higher up, and was attached to a vertical member of the shoulder attachment. It appears to provide a larger proportion of valid data sets, covering more Incline and Weight settings, with a smaller reduction in sampling rate. These are likely due to its position, reducing the chance of non-Line-of-Sight issues between it and the Base-Station, leading to fewer dropped packets. However, graphs of individual Z-Accelerometer output show more severe motions (Blue line on Fig. 16), likely due to play in the bolts previously mentioned leading to increased motion with respect to the sled. This may explain why it has proportionally more data files with errors outside the target of 0.1 m/s (8 out of 35 valid runs i.e. approximately 23 %) and why its RMSE value is higher. Of note, looking at the RMSE contour graph (Fig. 17), the worst results are achieved with the higher incline and lower weight settings, this may be due to shifting sled balance making it more likely to tip forward and backwards at each surge forward of the subject during the Pushing Phase.

The Front WIMU was located on a horizontal member located at the front upper part of the sled. It provides a lower proportion of valid data sets, covering fewer Incline and Weight settings, with a larger reduction in effective sampling rate. These are likely due to its low position which provides a greater chance of non-Line of Sight issues between it and the Base-Station leading to more dropped packets. Its Z-Accelerometer data also appears to have higher vibration and noise levels but far less severe motions during the Pushing Phase (see Fig. 15) which likely results in it having proportionally fewer data files with errors outside the target of 0.1 m/s (2 out of 24 valid runs i.e. approximately 8 %) and its slightly lower overall RMSE value. Looking at the contour graph (Fig. 18), high weight and low incline settings give the worst performance; this may be due to the added weight compressing the rubber wheels allowing more effective transmission of vibrations through the sled to the WIMU.

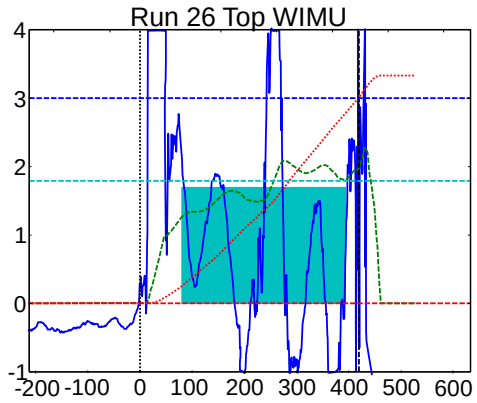

Fig. 16. Top WIMU has more severe accelerations.

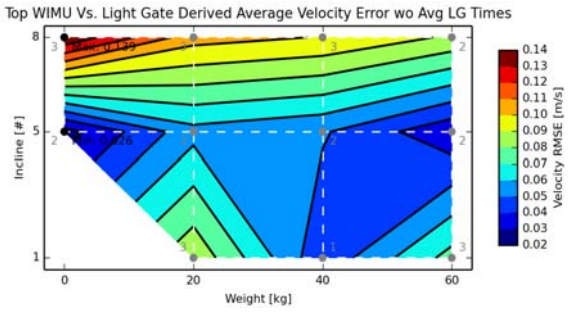

Fig. 17. Sled Average Velocity RMSE for Top WIMU showing greater coverage but worse overall performance.

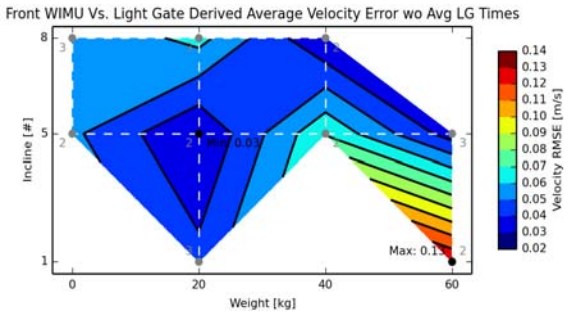

Fig. 18. Sled Average Velocity RMSE for Front WIMU showing worse coverage but better overall performance.

Although it appears that WIMU placement affects results, both WIMUs still provide accurate performance and have additional pros and cons. The effect of placement should be investigated further.

4.4. Other WIMU Derived Features

Although determination of sled Average Velocity from Z-Accelerometer PP data was the main focus of this investigation, a more complete analysis of the data from all sensors revealed other potentially useful information.

4.4.1. Step Detection

The cyclical nature of the Acceleration regime during the PP was believed to be related to the subject's gait, with each surge in Acceleration corresponding to the subject pushing against the ground with their feet at each step. As such, step counting was considered a possibility. This was attempted using filtering and peak detection methods on Z-Accelerometer data. Empirical tuning of variables allowed these features to be reliably detected. An example of output with Acceleration surges corresponding to each step highlighted in magenta for the Front WIMU in Run 22 is shown in Fig. 19, revealing 6 potential step features and attempting to quantify their contribution to sled forward motion.

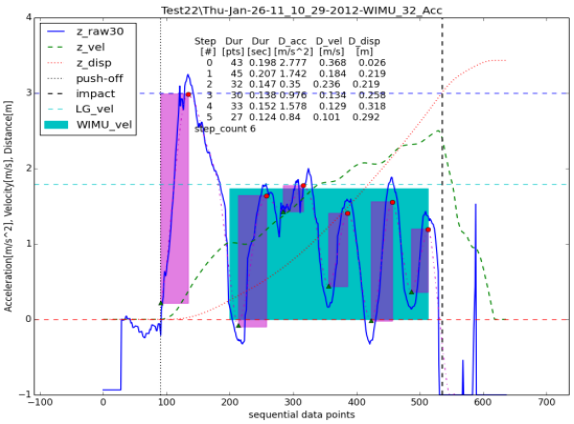

Fig. 19. Automated Detection of Steps (magenta).

However, validation of this process was not possible as it would require additional gait data such as from WIMUs worn on the subject's legs or synchronized video data.

4.4.2. Inclination Determination

The effect of gravity on the X & Z-Accelerometers could be used to estimate the track inclination. The PPO quiescent values from each sensor were estimated, then with an inverse tangent calculation both values were used to estimate Incline. The results for each WIMU were compared to the nominal Incline angle as well as that estimated Geometrically from measurements of the heights of each end of the 3 m Free Travel Length of the rails and presented in Fig. 20. Unfortunately, this was not as accurate as hoped with variability larger than the 1° required to distinguish between adjacent Incline settings. This poor accuracy was due to the limited amount of PPO data, the effect of motion artefacts, and high sensor noise levels. Furthermore WIMU placement seemed to affect the results, with the Top WIMU having larger values and higher errors than the Front WIMU, likely due to the mechanical play issues previously mentioned. Of note, the geometrically estimated and nominal Assassin incline values do not even match well, with a difference of approximately 1°, indicating inaccuracies in either the measurements taken, or the Assassin equipment itself due to imperfect manufacture, installation or excessive wear of components.

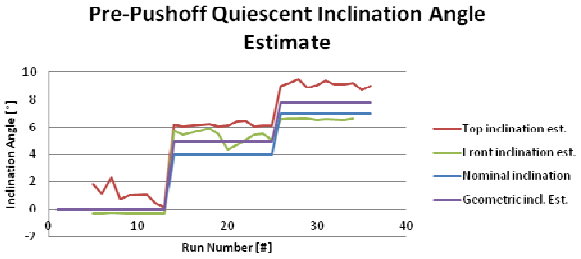

Fig. 20. Disagreement and variability of Calculated and Provided Assassin Incline Settings.

The effect of the geo-magnetic field on a magnetometer can also be used to estimate inclination. Normally this requires precise knowledge of the local field, careful calibration and compensation for Hard & Soft iron effects or local magnetic anomalies. Although the presence of magnetic disturbances such as the metal components of the Assassin mean simple conversion using laboratory calibration values and trigonometric calculations cannot be used to directly estimate the inclination angle, there were notable differences in PPO quiescent Z-Magnetometer values at each Incline setting. Of note, these were also far clearer

and less affected by noise than those from the Accelerometer. This can as can in Fig. 21 where the average of 100 PPO quiescent Z-Magnetometer values (blue) on the composite graph shows 3 distinct regions corresponding to each incline setting (green).

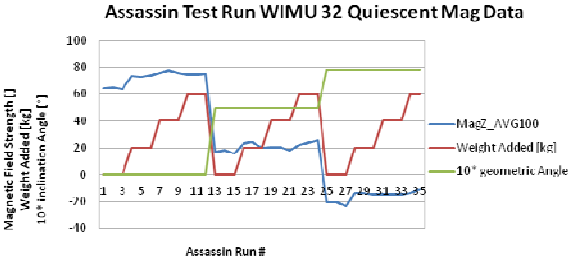

Fig. 21. Composite graph showing Magnetometer changes (Blue) for different Incline (Green) & Weight (Red) values.

4.4.3. Weight Detection

The PPO data for the initial, extra weight free, runs for each inclination displayed noticeably lower Z-Magnetometer values than subsequent runs at the same inclination with added weights (Fig 21). The weights added to the sled were made of cast iron and located near the Front WIMU; as such they affected the local magnetic regime enough to be detected by the WIMU's magnetometer. Even though the effect was smaller than magnetometer changes in response to incline change, and did not allow the number of weights added to be determined, this may still be of use to further automate the logging of training sessions.

5. Discussion

WIMU and Light-Gate derived Average Velocities are very similar, with most (42 of 52) data-files giving results within the target accuracy of 0.1 m/s. Much of this error can be attributed to limitations in the WIMU system such as noise on the Z-Accelerometer sensor, the lack of accurate per-sample time-stamps and occasional data loss. RMSE contour graphs reveal the worst results tend to be those with extreme combinations of Weight and Incline settings. Of note, as the estimated Light-Gate uncertainty levels are rather large, ranging from 0.06-0.115 m/s, it is possible that the WIMU system is performing better than indicated but is being masked by the uncertainty in the Light-Gate system derived results.

The validity of using a fixed ratio of timed region to full run duration to estimate sampling rate may be called into question as within a run, issues such as the loss of a radio packet, would affect the size of the timed and untimed portions depending on where it occurred. However, by using a large number of files and assuming events affecting effective sampling rate were randomly distributed this should still give a good approximation. There is also the possibility for a trend as velocity changes throughout the test as weight and incline changes as well as fatigue affect the ratio of durations for the timed and untimed periods. As first Weight and then Incline settings were progressively increased, this would be expected to lead to decreasing velocity, accentuated by subject fatigue. Such a trend was noted but it was not pronounced, so a fixed value was used. Using the final integrated data, the validity of this was checked by re-estimating this ratio. The result of 68.95 % was similar to the initial estimate of 67.7 %. Relying on an external data source may also be questioned but an improved future WIMU system would negate the need for this, using more accurate, per-sample time-stamping for direct determination of integration periods; or using on-board logging and processing to negate wireless data loss. These would remove the current implementation's reliance on the Light-Gates for estimating integration period.

Although a single accurate velocity value was the desired output of the system, it can be seen that the continuous stream of WIMU data provides a more complete picture of the Pushing-Phase. This could allow for more detailed analysis of the development of sled Velocity. Furthermore, it appears WIMU data can enable automated detection of individual steps, as well as Assassin Incline and Weight setting, however further validation of these is likely necessary.

The small-size, low-cost, portability and automation of the current system implies that future implementations could remove requirements for trained users, extensive sled modifications or costly installation of trackside equipment. This combined with similar investigations of other Push-Start training equipment and other sports disciplines implies that these could be used to track performance across gym, test-track and on-ice sleds. Such a system holds great potential for: improving the understanding of the Push-Start; identifying good athletes and determining the effectiveness of coaching and training interventions.

6. Conclusions

Using WIMUs to instrument the Assassin Push-Start Trainer, an automated method for determining average velocity was developed. Sled Average Velocity results were similar to those gathered using an existing Light-Gate system with Root Mean Squared Error within or similar to the target accuracy level of 0.1 m/s. Furthermore, it seems possible to automatically determine other useful information such as step count, equipment Incline and whether extra Weight has been added, allowing for an almost completely automated method of logging a training session. The system's accuracy, low-cost, ease-of-use and portability, could provide greater access to such quantitative performance data, with its highly

detailed data enabling improved understanding of the Push-Start. These could lead to improved methods for Selection, comparison and training, potentially providing a valuable competitive edge.

7. Future Work

Although the system developed delivers estimates of sled velocity comparable to the existing Light-Gate method, several avenues have been identified for further development. These cover improvements to WIMUs, the test setup, and additional data gathering.

Improved WIMU hardware can address many of the issues encountered. Sensors with lower noise & higher sample rates could improve the accuracy of initial integration results. Improved radio systems with higher throughput may be needed to support these higher data rates, furthermore improved radios could also allow for reduced packet loss by being able to handle acknowledgements and re-transmits while still maintaining high throughput, further improving accuracy. Alternatively the use of data storage, time-stamping and an improved processor in WIMU hardware could allow data gathering and processing to be performed on-board, removing much of the reliance of RF and its associated issues. On-going developments to Tyndall's WIMU capabilities mean many of these features have already been developed.

Improvements to the test setup could also be targeted. These could include better attachment locations and methods for the WIMUs to reduce vibration and motion artefacts; as well as adding in-the-field calibration stages to further improve WIMU sensor accuracy.

Perhaps the most important aspect would be to perform more tests using additional equipment-setups and athletes. These are necessary to confirm that the method is fit for use across a wide range of scenarios such as: different pushing attachments; subject experience level; gender; and technique, as these may provide very different motion patterns. Furthermore, the use of additional data sources and measurements for validation of WIMU data would be useful, such as: extra WIMUs on the subject's legs; and synchronized high-speed video.

It is hoped that this will allow development of a self-contained, low-cost, single-device system that can be used to monitor performance of athletes in various sledding sports from the gym to the track resulting in improved selection, coaching & training.

Acknowledgements

We would like to acknowledge the support of Science Foundation Ireland (SFI) in funding the CLARITY Centre for Sensor Web Technologies under grant 07/CE/I1147, and the technical and financial assistance of the University Of Bath and UK Sports in this deployment.

References

[1]. C. Zanoetti, A. La Torre, G. Merati, E. Rampinini, F. M. Impellizzeri, Relationship between push phase and final race time in skeleton performance, *The Journal of Strength & Conditioning Research*, Vol. 20, Aug. 2006, pp. 579-583.

[2]. W. A. Sands, *et al*., Skeleton: Anthropometric and physical abilities profiles: US national skeleton team, *Sports Biomechanics*, Vol. 4, Jul. 2005, pp. 197-214.

[3]. FIBT Bob-Skeleton Results. Available: www.fibt.com/races-results/results.html, Retrieved: September 2014.

[4]. FIBT International Skeleton Rule 16.9 - Starting Area: Bobsleigh and Skeleton, *FIBT*, 2009. Available: http://www.fibt.com/fileadmin/Rules/Reg SKELETON-2009 - E.pdf, Retrieved: Sep. 2014.

[5]. N. Bullock, W. G. Hopkins, D. T. Martin, F. E. Marino, Characteristics of performance in skeleton World Cup races, *Journal of Sports Sciences*, Vol. 27, Feb. 2009, pp. 367-372.

[6]. C. Cook, D. Holdcroft, S. Drawer, L. P. Kilduff, Designing a warm-up protocol for elite bob-skeleton athletes, *International Journal of Sports Physiology & Performance*, Vol. 8, Mar. 2013, pp. 213-215.

[7]. S. Colyer, Consecutive Days of Push Start Testing May Mask the Effect of Starting Style In Skeleton - a Pilot Study, in *Proceedings of the 27th Easter Meeting of the BASES Biomechanics Interest Group (BIG'12)* University of Ulster, Belfast, Northern Ireland, April 2012.

[8]. N. Bullock, *et al*., Characteristics of the start in women's World Cup skeleton, *Sports Biomechanics*, Vol. 7, September 2008, pp. 351-360.

[9]. S. Lembert, O. Schachner, C. Raschner, Development of a measurement and feedback training tool for the arm strokes of high-performance luge athletes, *Journal of Sports Sciences*, Vol. 29, Nov. 2011, pp. 1593-1601.

[10]. F. Braghin, F. Cheli, M. Donzelli, S. Melzi, E. Sabbioni, Multi-body model of a bobsleigh: comparison with experimental data, *Multibody System Dynamics*, Vol. 25, Aug. 2010, pp. 185-201.

[11]. USA-Bobsled-Skeleton-Federation. Combine Test Protocol. Available: www.teamusa.org/USA-Bobsled-Skeleton-Federation/, Retrieved: Sep. 2014.

[12]. N. Bullock, *et al.*, Talent identification and deliberate programming in skeleton: Ice novice to Winter Olympian in 14 months, *Journal of Sports Sciences*, Vol. 27, 2009, pp. 397-404.

[13]. C. Valle, Think you want to be a bobsledder? Available: http://www.freelapusa.com/think-you-want-to-be-a-bobsledder/, Retrieved: September 2014.

[14]. M. Gaffney, M. Walsh, B. O'Flynn, C. Ó Mathúna, Accurate Sled Velocity on a Short-Inclined Track Using Accelerometer Data, in *Proceedings of the Eighth International Conference on Sensor Technologies and Applications (SENSORCOMM'14)*, Lisbon, Portugal, 16-20 November 2014, pp. 169-174.

[15]. M. Gaffney, M. Walsh, B. O'Flynn, C. Ó Mathúna, Derivation of Velocity/Distance Curves from a Wireless Inertial Measurement Unit Instrumented

Bob-Skeleton Sled and Comparison to Light-Gate and Video Derived Values, *British Journal of Sports Medicine*, Vol. 47, No. 17, 2013, pp. e4-e4.
[16]. B. O'Flynn, *et al.*, The development of a novel minaturized modular platform for wireless sensor networks, in *Proceedings 4th International Symposium on Information Processing in Sensor Networks (IPSN),* April 2005, pp. 370-375.
[17]. J. Barton, *et al*., Miniaturised inertial measurement units for wireless sensor networks & novel display interfaces, in *Proceedings 55th Electronic Components & Technology Conference (ECTC)*, June 2005, pp. 1402-1406.
[18]. J. Barton, A. Gonzalez, J. Buckley, B. O'Flynn, S. C. O'Mathuna, Design, Fabrication and Testing of Miniaturised Wireless Inertial Measurement Units (IMU), in *Proceedings 57th Electronic Components & Technology Conference (ECTC)*, May 2007, pp. 1143-1148.
[19]. C. Rodde, A Wireless Inertial Measurement System for Tennis Swing Dynamics, MEngSc (Microelectronic design) Taught Masters, *Department of Microelectronic Engineering, University College Cork (UCC) and Tyndall National Institute*, Cork, 2009.
[20]. M. Gaffney, *et al.*, Wearable wireless inertial measurement for sports applications, in *Proceedings 33rd IMAPS-CPMT*, Gliwice–Pszczyna, Poland, September 2009, pp. 138-141.
[21]. M. Gaffney, *et al*., A Smart Wireless Inertial Measurement Unit System, in *Proceedings of the Presented at Pervasive Health Conference,* UCD, Dublin, Ireland, May 2011.
[22]. M. Gaffney, M. Walsh, B. O'Flynn, C. O Mathuna, An automated calibration tool for high performance Wireless Inertial Measurement in professional sports, in *Proceedings of the IEEE Sensors Conference*, Limerick, Ireland, October 2011, pp. 262-265.
[23]. Brower Timing Systems, Test Centre (TC) Timing System. Available: www.browertiming.com, Retrieved: September 2014.